

Normalized-lifetime thermal-lens method for the determination of luminescence quantum efficiency and thermo-optical coefficients: Application to Nd³⁺-doped glasses

C. Jacinto,^{1,*} S. L. Oliveira,¹ L. A. O. Nunes,¹ J. D. Myers,² M. J. Myers,² and T. Catunda^{1,†}
¹*Instituto de Física de São Carlos, Universidade de São Paulo - USP, CEP 13560-970, São Carlos - SP, Brazil*
²*Kigre Inc., 100 Marshland Road, Hilton Head Island, South Carolina 29926, USA*
 (Received 29 November 2005; published 14 March 2006)

We present a new method based on thermal lens (TL) technique to determine the fluorescence quantum efficiency, η , and thermo-optical coefficients of fluorescent materials. These parameters can be obtained from the linear dependence of the TL signal with the experimental lifetimes of a set of samples with different luminescent ion concentrations. The method was applied in Nd³⁺-doped materials (Q-98 Phosphate, fluorozirconate, and fluorindate). The obtained values are in agreement with those determined by other approaches based on TL methods and the ratio between experimental and radiative lifetime values (Judd-Ofelt theory). The method hereafter presented is very simple and does not require comparison with a reference sample or the use of multiple excitation wavelengths. In addition, the nature of concentration quenching taking into account the achieved η and τ values and respective energy transfer microparameters, is discussed.

DOI: [10.1103/PhysRevB.73.125107](https://doi.org/10.1103/PhysRevB.73.125107)

PACS number(s): 78.20.Nv, 78.55.-m, 78.90.+t, 78.60.-b

I. INTRODUCTION

Among the most important parameters that drive the performance of solid-state lasers are the thermal conductivity, K , the temperature coefficient of the optical path length, ds/dT , and the fluorescence quantum efficiency, η . The last is defined as the ratio of the number of radiative deexcitations to the total number of deexcitations of an energy state in a given system. The determination of the absolute value of η in luminescent ion-doped solids has been shown to be a challenging task, particularly in solids. Several methods have been used to measure η , including pure optical measurements such as using integrating spheres, comparing the measured and radiative lifetime values of the investigated energy state and employing photothermal methods such as photoacoustic, photocalorimetry, photopyroelectric, and thermal lens (TL).¹⁻¹⁸ Various methods provide good results but some of them require relatively complicated experimental setups, the need of absolute photodetector calibration, knowledge of absolute concentrations of impurity ions, and the availability of a suitable standard.

Another very important parameter is ds/dT , since it describes the thermally induced distortion of a laser beam during its passing through an absorbing medium. To obtain efficient solid-state lasers, the active medium, usually made of doped glasses or crystals, needs to have a high radiative emission rate and low thermal lens effect, which means that ds/dT needs to be near zero.^{18,19}

In this paper, we present a new approach to determine η and thermo-optical coefficients of fluorescent materials using

the TL technique. This approach was originally proposed by Quimby and Yen in a photoacoustic experiment.⁸ However, in photoacoustics it is very difficult to compare data of different samples because the acoustic coupling between sample and sensor can vary.^{1,6} The new methodology presented in this paper requires only measurements of the photothermal signal and fluorescence lifetimes of a collection of samples with several ion concentrations in the same host matrix composition. We applied this method to Nd³⁺ doped glasses and the obtained results compared very well with previous measurements,^{16,17} and the ratio of measured and radiative lifetimes (Judd-Ofelt).^{20,21} In addition, the fluorescence concentration quenching effect is discussed based on the achieved η and τ values and respective energy transfer microparameters. For convenience the variables used in this work are listed in the appendix.

II. THEORETICAL BACKGROUND

A. Thermal lensing

The TL technique is based on the induced TL effect in a partially transparent medium when an excitation laser beam passes through the sample. The laser induced temperature profile $\Delta T(r, t)$ leads to an optical path profile, which is approximately equivalent to that of a lens. The propagation of a probe beam through this TL results in a variation of its on-axis intensity, $I_{\text{TL}}(t)$, which can be calculated with diffraction integral theory, and that was derived in Ref. 22 and adapted for solid samples in Ref. 23, as

$$\frac{I(t)}{I(0)} = \left\{ 1 - \frac{\theta}{2} \tan^{-1} \left[\frac{2mV}{[(1+2m)^2 + V^2]_t} \sqrt{2t + 1 + 2m + V^2} \right] \right\}^2, \quad (1)$$

where

$$m = \left(\frac{w_p}{w_{ex}} \right)^2, \quad V = \frac{Z_1}{Z_c} \quad (\text{when } Z_c \ll Z_2). \quad (2)$$

here, Z_c is the confocal distance of the probe beam, Z_1 is the distance between the probe beam waist and the sample, Z_2 is the distance between the sample and the photodiode, w_p and w_{ex} are the probe and excitation radii at the sample, $I_{TL}(t)$ is the temporal dependence of the laser beam at the detector, and $I_{TL}(0)$ is the initial value of $I_{TL}(t)$. The temporal evolution of the TL signal depends on the characteristic time, t_c , which is related to the thermal diffusivity (D) by $t_c = w_{ex}^2/4D$.¹⁷

In the TL method, the fit of experimental data with Eq. (1) provides two quantitative parameters: D and θ . The parameter θ is proportional to the probe beam phase shift induced by the thermal lens. In most cases it is convenient to normalize θ by the absorbed pump power, P_{abs} , which is given by

$$\Theta = -\frac{\theta}{P_{abs}} = \frac{1}{K\lambda_p} \frac{ds}{dT} \varphi, \quad (3)$$

where λ_p is the probe beam wavelength, $K = \rho c D$ is the thermal conductivity, ρ is the density, c is the specific heat, ds/dT is the temperature coefficient of the optical path length change at the probe beam wavelength, and φ is the fraction of absorbed energy converted into heat. In fluorescent materials, part of the absorbed excitation is converted into heat and the remaining energy is converted in fluorescence. Considering that $h\nu_{ex}$ is the excitation photon energy and $h\langle\nu_{em}\rangle$ is the average energy of the emitted photon, thus the fluorescence quantum efficiency, η , can be obtained from φ through the following relation:¹⁴⁻¹⁸

$$\varphi = 1 - \eta \frac{\langle\nu_{em}\rangle}{\nu_{ex}}. \quad (4)$$

Regarding ds/dT , for solid samples it is given by three contributions: dn/dT , end-face curvature, and thermal stress. For the case of thin disk geometry, i.e., the sample thickness much smaller than diameter, the expression for ds/dT considering these three contributions is given by^{15,17,19}

$$\frac{ds}{dT} = \frac{dn}{dT} + \alpha(n_0 - 1)(1 + \nu) + \frac{n_0^3}{4} Y \alpha (q_{\parallel} + q_{\perp}), \quad (5)$$

where α is the linear thermal-expansion coefficient, n_0 is the refractive index, ν is the Poisson ratio, Y is the Young modulus, q_{\parallel} and q_{\perp} are the stress-optical coefficients for the parallel and perpendicular orientation relative to excitation beam polarization (for crystals). The second term on the right-hand side of Eq. (5) represents the end-face curvature due to larger expansion of the hotter center compared to the edge of the sample. The fact that the cooler part of the sample prevents expansion of its hotter center generates thermal stress, given by the third term in Eq. (5). It should be noted that the quantity ds/dT is normalized by the sample length L , so that calling S the sample optical path, $ds/dT = L^{-1} dS/dT$. In the literature, $ds/dT = dn/dT + (n_0 - 1)\alpha$ is usually found, which is valid for a uniformly distributed temperature rise. Therefore, the terms $(1 + \nu)$ and the stress-

optical coefficients, appear due to the lenslike shape of TL temperature profile.

B. Normalized lifetime method for determination of η and ds/dT

The methodology proposed in this work for determination of η and ds/dT is based on the relationship between η and the fluorescence lifetimes (τ) of a collection of samples with different ion concentrations. This connection is given by $\eta = A_{rad}/W_T = \tau/\tau_{rad}$, where $A_{rad} = \tau_{rad}^{-1}$ is the radiative emission rate and $W_T = \tau^{-1}$ is the total decay rate, which includes all radiative and nonradiative processes. In practice, the fluorescence decay may be nonexponential so that an effective lifetime value, τ_{eff} , must be calculated from the fluorescence decay signal, $I_F(t)$, by¹⁰

$$\tau_{eff} = \frac{1}{I_F(0)} \int_0^{\infty} I_F(t) dt. \quad (6)$$

Due to the concentration quenching effect, $\eta(N_i)$ and $\tau(N_i)$ depend strongly on ion concentration (N_i). Taking into account that $\eta = \tau/\tau_{rad}$, we can write $\eta(N_i) = \eta^* \Gamma(N_i)$, where $\Gamma(N_i) = \tau/\tau^*$ is the normalized lifetime parameter and η^* is the fluorescence quantum efficiency of one sample of the set of concentrations, whose lifetime is τ^* .⁸ Therefore, a linear relationship between Θ and Γ is obtained from Eqs. (3) and (4),

$$\Theta = C \left(1 - \Gamma \eta^* \frac{\langle\nu_{em}\rangle}{\nu_{ex}} \right), \quad (7)$$

where $C = (\lambda_p K)^{-1} (ds/dT)$. Equation (7) indicates that both C and η^* can be obtained from the plot of $\Theta(N)$ versus $\Gamma(N)$, determined by TL and lifetime measurements, respectively. In addition, the fluorescence quantum efficiencies for all sets of concentrations is obtained from the relation $\eta(N_i) = \eta^* \Gamma(N_i)$; and ds/dT is calculated from C . It is important to point out that this method assumes that τ_{rad} , C , and $\langle\nu_{em}\rangle$ are independent of ion concentration, which is a reasonable assumption for diluted rare earth doped glasses and crystals. Hereafter, this method will be called normalized lifetime (NL) method.

Nd³⁺-doped materials are excellent systems to check the merit of this method, since their fluorescence mechanisms are extensively studied in many systems,²⁴ and normally they present only one important fluorescence channel (${}^4F_{3/2} \rightarrow {}^4I_J$ multiplets with $J = 15/2, 13/2, 11/2,$ and $9/2$). The average emission frequency can be estimated by $\langle\nu_{em}\rangle = \sum_J \beta_J (\nu_{em})_J$, where the branching ratios, β_J , are obtained from luminescence measurements.

C. Fluorescence concentration quenching and energy transfer parameters

The interaction between pairs of Nd³⁺ plays an important role in the quantum efficiency of ${}^4F_{3/2}$ level. By increasing the Nd concentration, a decrease of the fluorescence lifetime is usually observed. This is the so-called fluorescence concentration quenching effect. This reduction is attributed to

cross relaxation (CR) processes, which are enhanced by energy migration (EM).^{10,24,25} The result is the conversion of part of the original excitation energy into heat, i.e., an increase of the thermal load. The fluorescence concentration quenching effect of Nd³⁺ doped materials has been described by the following expression of fluorescence time decay from the ⁴F_{3/2} level:¹⁰

$$I_F(t) = I_F(0)\exp(-W_{\text{exp}}t - \gamma\sqrt{t}), \quad (8)$$

where I_F is the ⁴F_{3/2} level fluorescence, which is composed by an exponential term (W_{exp}) and the classic Förster^{10,26,27} decay function [$\exp(-\gamma\sqrt{t})$], also known as static disordered decay. $W_{\text{exp}} = A_{\text{rad}} + W_0 + W_{\text{CR}}$, in which W_0 is the nonradiative relaxation rate due to multiphonon emission and W_{CR} accounts for CR that is enhanced by EM. The Förster term describes CR without EM. A_{rad} and W_0 are independent of Nd³⁺ concentration, while both γ and W_{CR} are concentration dependent. However, only γ leads to a deviation from the purely exponential behavior of the decay. This fact is in general attributed to different distances between donors and acceptors, leading to decay rates that differ for each donor-acceptor pair. The resulting overall decay is then nonexponential, with an initial faster decay due to sites with smaller separation between pairs.

Energy transfer between ions is generally described on the basis of dipole-dipole interaction.^{10,27} The transfer rate from a donor D to an acceptor A is governed by the so-called energy transfers microparameters C_{DA} and C_{DD} . For Nd³⁺ ions the processes involved in the CRs are ⁴F_{3/2}, ⁴I_{9/2} → ⁴I_{15/2}, ⁴I_{15/2} and/or ⁴F_{3/2}; ⁴I_{9/2} → ⁴I_{13/2}, ⁴I_{15/2} for C_{DA} ; and in the EM is ⁴F_{3/2}, ⁴I_{9/2} → ⁴I_{9/2}, ⁴F_{3/2} for C_{DD} . These parameters can be obtained from the Dexter model by means of the spectral overlap between the donor emission (σ_D^{em}) and the acceptor (σ_X^{abs}) absorption cross section given by¹⁰

$$C_{DX} = \frac{3c}{8\pi^4 n_0^2} \int \sigma_D^{\text{em}}(\lambda) \sigma_X^{\text{abs}}(\lambda) d\lambda, \quad (9)$$

where c is the velocity of light and n_0 is the refractive index of the medium.

According to the Förster model,²⁶ γ can be determined by

$$\gamma = \frac{4}{3} \pi^{3/2} N_t \sqrt{C_{DA}} \quad (10)$$

Burshtein²⁸ introduced the hopping model to account for EM among donors with a rate given by

$$W_{\text{CR}} = \pi \left(\frac{2\pi}{3} \right)^{5/2} \sqrt{C_{DA} C_{DD} N_t^2} = A_{\text{rad}} n^2. \quad (11)$$

Equations (10) and (11) were purposely written for the specific case of singly doped materials, where donor (N_D) and acceptor (N_A) species are the same, i.e., $N_D = N_A = N_t$, which in this work is the total Nd³⁺ concentration. In Eq. (11) we introduced two parameters, the normalized concentration $n = N_t/N_c$ and the critical density $N_c = [A_{\text{rad}}^2 / \pi^2 (2\pi/3)^5 C_{DD} C_{DA}]^{1/4}$, where N_c is defined from Eq. (11) with the condition $W_{\text{CR}}(N_c) = A_{\text{rad}}$.

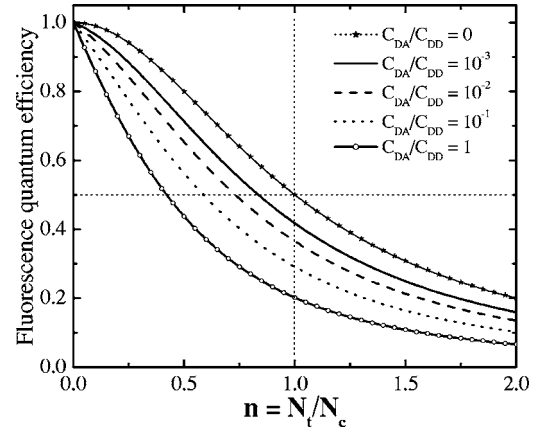


FIG. 1. Concentration quenching effect on the fluorescence quantum efficiency for several C_{DA}/C_{DD} values. In all curves $\eta_0 = 1$, i.e., $W_0 = 0$ was used. The n parameter is related to the N_t/N_c .

Since the decay kinematics described by Eq. (8) are nonexponential, in order to calculate the fluorescence quantum efficiency we used $\eta = \tau_{\text{eff}}/\tau_{\text{rad}}$, with τ_{eff} being defined by Eq. (6). This procedure results in

$$\eta = \frac{\int_0^\infty I(t) dt}{\int_0^\infty I(0) \exp(-A_{\text{rad}} t) dt} = \frac{F(x)}{\eta_0^{-1} + n^2} \quad (12)$$

in which

$$F(x) = \{1 - \sqrt{\pi} x \exp(x^2) [1 - \text{erf}(x)]\}, \quad (13a)$$

$$x^2 = \frac{\gamma^2}{4W_{\text{exp}}} = \sqrt{\frac{3}{2\pi} \frac{C_{DA}}{C_{DD}}} \frac{n^2}{(\eta_0^{-1} + n^2)} \quad (13b)$$

and $\eta_0 = A_{\text{rad}}/(A_{\text{rad}} + W_0)$ is the fluorescence quantum efficiency for zero Nd concentration limit (absence of concentration quenching), $\text{erf}(x)$ is the error function, and x is a quantity related to the ratio between the nonexponential and exponential decay terms in Eq. (8).

Both $I_F(t)$ and $\eta(n)$ critically depend on the parameters C_{DA} and C_{DD} . In order to illustrate this behavior, Fig. 1 shows a plot of η versus n for several values of the ratio C_{DA}/C_{DD} , for the case $\eta_0 = 1$ ($W_0 = 0$). For $C_{DA} \ll C_{DD}$, $x \rightarrow 0$ and $F(x) \rightarrow 1$, it should be noticed that

(i) $\gamma^2 \ll W_{\text{exp}}$, so that $I_F(t)$ should be nearly exponential with decay time $\tau = W_{\text{exp}}^{-1}$ (the nonexponential behavior increases when x increases).

(ii) $W_{\text{exp}} = (\eta_0^{-1} + n^2) W_{\text{rad}}$ increases quadratically with concentration and $\eta(n) = (\eta_0^{-1} + n^2)^{-1}$.

(iii) $\eta(n)$ has zero slope at $n=0$. It becomes negative when C_{DA} increases.

(iv) $\eta(n) = \eta_0/2$ for $n=1$ ($N_t = N_c$).

It is interesting to define the factor q by the condition $\eta(q) = \eta_0/2$. According to Fig. 1 $q=1$ only when $C_{DA}=0$ and q decreases as C_{DA}/C_{DD} increases. From the data presented

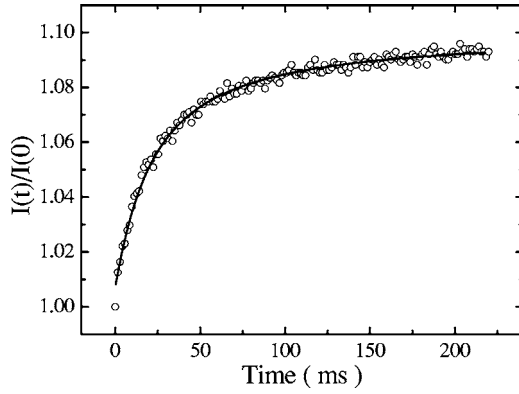


FIG. 2. TL transient signal for Q-98 sample doped with 1.1×10^{20} $\text{Nd}^{3+}/\text{cm}^3$, at $\lambda_{\text{ex}}=801.6$ nm and excitation power of 180 mW. The curve fitting provided $\theta = -(0.0933 \pm 0.0003)$ rad and $t_c = (3.96 \pm 0.04)$ ms.

in Fig. 1, $q=0.83$, 0.73 , 0.58 , and 0.42 for $C_{DA}/C_{DD} = 10^{-3}$, 10^{-2} , 10^{-1} , and 1 , respectively.

The spectroscopy properties of Nd^{3+} doped crystals and glasses have been extensively explored in the literature.^{19,24,27,29,30} It is important to remark that for glasses, the variations of local field from site-to-site causes an inhomogeneous broadening in the absorption and emission spectra. Consequently, the fluorescence decay can be nonexponential owing to the statistical distribution of A_{rad} . This behavior is expected even in the absence of interactions between ions (low concentration limit) although energy transfer can also contribute to the nonexponential decay character. In the great majority of works, the quantum efficiency of Nd^{3+} doped glasses has been calculated by $\eta_{\text{JO}} = \tau_{\text{exp}}/\tau_{\text{rad}}$, where τ_{exp} is the measured decay time and τ_{rad} is calculated by Judd-Ofelt method.^{5,31} The so-called, JO parameters are obtained through the oscillators strengths of Nd absorption bands. Therefore, this method requires the knowledge of ion concentration. In some cases, the quantum efficiencies were directly determined by photoacoustics,^{6–8} calorimetry¹¹ or integrating sphere^{9,10,32} methods. As an example, we consider a Nd^{3+} doped LG-750 glass, where $\tau_{\text{rad}}=352$ μs and $\tau_0 = 377$ μs (Ref. 10) (τ_0 is the experimental lifetime observed in a very diluted sample, so that concentration quenching effects are negligible). This inconsistency, $\tau_0 > \tau_{\text{rad}}$, indicates an overestimation of A_{rad} , which is often obtained in phosphate glasses.^{29,30} Using an integration sphere method, Caird *et al.*¹⁰ obtained $\eta_0 = 0.91 \pm 0.05$ for LG-750, in the low concentration limit. This result indicates $\tau_{\text{rad}} \approx \tau_0/0.91 = 414$ μs , which is $\sim 17\%$ higher than $\tau_{\text{rad}}=352$ μs obtained by JO. This 17% of discrepancy is within the generally estimated accuracy of JO method $\sim 15\% - 20\%$.^{5,14,31}

Fluorescence quenching is also commonly studied by measuring the concentration dependence of the measured e^{-1} , the first e -fold decay time, $\tau_1(N_i)$. For some kinds of ultraphosphates and silicates, the quenching effect is better fit by a linear function, $\tau_1 = \tau_0(1 - N_i/Q)$, which gives a non-zero slope for $\eta(N_i)$ at the origin.³² However, the experimental data is usually adjusted by the empirical expression:^{24,27,29,30}

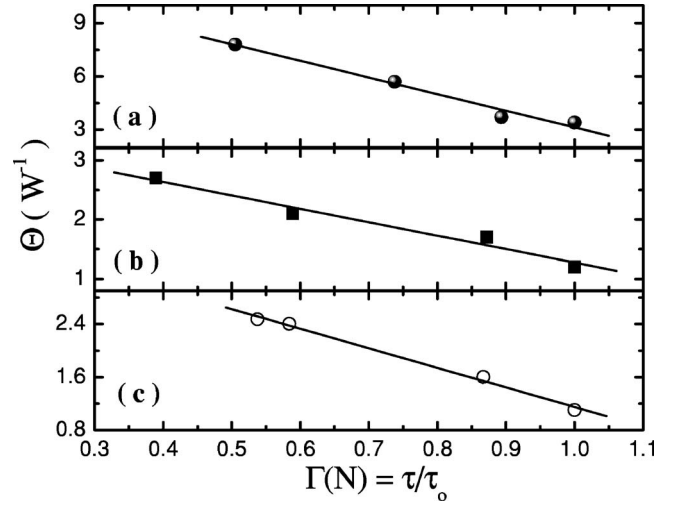


FIG. 3. Dependence of photothermal parameter Θ with the normalized lifetime $\Gamma(N) = \tau/\tau^*$, where τ^* is the lifetime of the sample with lowest ion concentration, for sets of Nd^{3+} doped glasses: (a) fluorozirconate (ZBLAN); (b) fluoroindate (PGIZCa); and (c) phosphate (Q-98). The excitation wavelengths used were 796 nm for (a) and (b) and 801.6 nm for (c).

$$\tau_1^{-1} = \tau_0^{-1} \left[1 + \left(\frac{N_i}{Q} \right)^p \right], \quad (14)$$

where τ_0 is the e^{-1} decay time observed in very diluted samples, Q is the concentration where $\tau(Q) = \tau_0/2$, and p is an adjustable parameter. It is generally assumed that $p \approx 2$. Indeed, for pure exponential decay Eq. (11) predicts $p=2$ since $W_{\text{CR}} \propto N_i^2$.²⁷ A very good agreement with $p=2$ behavior was observed in phosphates (LG-770, LHG-8), some ultraphosphates, and fluoride glasses.^{25,33,34} The Q parameter (in units of 10^{20} cm^{-3}) varies between 5–10 for phosphates and ultraphosphates and 4–8 for fluorides.^{24,33} Based on data of a series of multicomponent metaphosphate glasses, Payne *et al.*³⁵ observed that Q decreases linearly with the emission bandwidth.

III. EXPERIMENT

The glasses studied in this work were Phosphate (Q-98), Fluorozirconate (ZBLAN), and fluoroindate (PGIZCa) doped with different Nd concentrations. The glass composition of ZBLAN and PGIZCa glasses were described previously^{16,17} and the phosphate glasses were manufactured by Kigre Inc.

Infrared fluorescence measurements were made to determine $\langle \nu_{\text{em}} \rangle$ using a diode laser operating at 808 nm as pumping source, and a Czerny-Turner monochromator coupled with an InGaAs detector to record the signal. The lifetimes of ${}^4F_{3/2}$ level were determined using a Ti:Sapphire laser at 808 nm modulated by a mechanical shutter. The transient signal was dispersed by the monochromator and recorded in a digital oscilloscope. The lifetime values were achieved using Eq. (6). We also determined the lifetime by a single exponential fit of the decay signal and the results showed a good agreement ($\pm 5\%$) with the effective values obtained through Eq. (6).

TABLE I. Comparison of the parameters C and ds/dT obtained from the methods: reference sample (RS), multiwavelength (MW), and normalized lifetimes (NL).

Sample	$C=(\lambda_p K)^{-1} ds/dT (W^{-1})$			ds/dT ($10^{-6} K^{-1}$)
	RS	MW	NL	
Q-98 (Kigre)		3.9 ± 0.1	4.1 ± 0.1	1.31 ± 0.03
ZBLAN	-13.3 ± 0.3	-13.7 ± 0.9	-12.5 ± 0.8	-6.1 ± 0.4
PGIZCa	-3.6 ± 0.2	-3.6 ± 0.1	-3.7 ± 0.1	-2.4 ± 0.1

The dual beam mode mismatched TL experimental setup used here is also described in detail elsewhere.^{17,23} The measurements were performed using a Ti:Sapphire and He-Ne (632.8 nm) lasers as excitation and probe beams, respectively. The cw Ti:Sapphire laser was tuned about 800 nm, in resonance with the (${}^5F_{5/2}, {}^2H_{9/2}$) level of Nd^{3+} , whence non-radiative decays occur to the ${}^4F_{3/2}$ state. This is the most efficient way of populating the ${}^4F_{3/2}$ metastable state in diode pumped solid state lasers (DPSSL).

IV. RESULTS AND DISCUSSION

A. Fluorescence quantum efficiency and thermo-optical coefficient

Figure 2 shows a typical TL transient signal for the Q-98 sample doped with $1.1 \times 10^{20} Nd^{3+}/cm^3$. The solid curve represents the fit curve obtained from Eq. (1), which provides the θ and t_c values, where $m=10.54$ and $V=1.73$ were used as fix parameters. As an example, using the obtained t_c value in the relation $t_c = w_{ex}^2/4D$, jointly with the w_{ex} value used in the experiment, it is possible to determine D

$= (2.2 \pm 0.1) \times 10^{-3} cm^2/s$. In order to determine the η values, $\Theta = -\theta/P_{abs}$ was obtained, for each sample, from the plot of θ versus P (excitation power). Care was taken to work in the low excitation regime, in order to avoid nonlinear effects such as absorption saturation or Auger upconversion, owing to pairs interaction.^{18,36,37} Therefore, a linear dependence of θ versus P was observed in all measurements and the slopes of these curves were used to obtain θ/P and then Θ .

Although the choice of the reference sample (that one with lifetime τ^* and quantum efficiency η^*) is arbitrary, we choose the sample with lowest Nd concentration, for the three sets of glasses in this work. Consequently, the samples with $\Gamma=1$ have higher η and lower Θ . Figure 3 shows that Θ decreases linearly with Γ as predicted by Eq. (7). This behavior validates the assumptions made in the method, τ_{rad} and C are independent of the concentration and $\eta(N_t) \propto \tau(N_t)$. The η^* and C parameters were determined from the linear fit of Fig. 3 data, jointly with the values of ν_{ex} and $\langle \nu_{em} \rangle$. ds/dT and $\eta(N_t)$ were achieved by means of $C = (\lambda_p K)^{-1} ds/dT$ and $\eta(N_t) = \eta^* \Gamma(N_t)$, respectively. Table I shows C and ds/dT values for studied glasses, and Table II presents the η values for all concentrations. It is relevant to point out that identical values of $\eta(N_t)$ and C are obtained if any sample of the set of concentrations is used as reference.

To better evaluate the NL method, other experiments have been carried out to compare the results obtained by this method with other approaches also based on TL technique: the multiwavelength (MW)^{15,16} and the reference sample (RS)^{14,17} methods. The MW method explores the linear dependence of Θ with the excitation wavelength, $\Theta = C(1 - \eta(\lambda_{em}^{-1})\lambda_{ex})$, obtained from Eqs. (3) and (4). This idea of using the linear dependence of the photothermal signal with λ_{ex} has already been explored in other photothermal tech-

TABLE II. Measured fluorescence quantum efficiencies values obtained from the Judd-Ofelt analysis and TL technique using reference sample (RS), multiwavelength (MW), and normalized lifetimes (NL) methods.

Sample	N_t ($10^{20} cm^{-3}$)	αL^a	τ (μs)	Fluorescence quantum efficiency			
				JO	RS $\pm 15\%$	MW	NL $\pm 10\%$
Q-98 (Kigre)	1.1	0.66	346	0.88		0.91 ± 0.05	0.90
	3.3	1.48	300	0.77			0.78
	6.7	2.62	202	0.52			0.53
	10.3	4.70	186	0.47			0.48
ZBLAN	0.9	0.41	515	1.03	0.99	0.99 ± 0.03	0.99
	1.9	0.64	460	0.92	0.80		0.88
	3.5	1.26	380	0.76	0.65		0.73
	5.2	1.74	260	0.52	0.49		0.50
PGIZCa	1.2	0.58	421	0.94	0.94		0.89
	2.3	0.98	367	0.82	0.80	0.76 ± 0.03	0.78
	4.2	1.85	248	0.55	0.67		0.52
	6.5	3.02	164	0.37	0.48		0.48

^a α is the optical absorption coefficient at λ_{ex} used in the TL experiment, and $L \sim 0.2$ cm is the sample thickness.

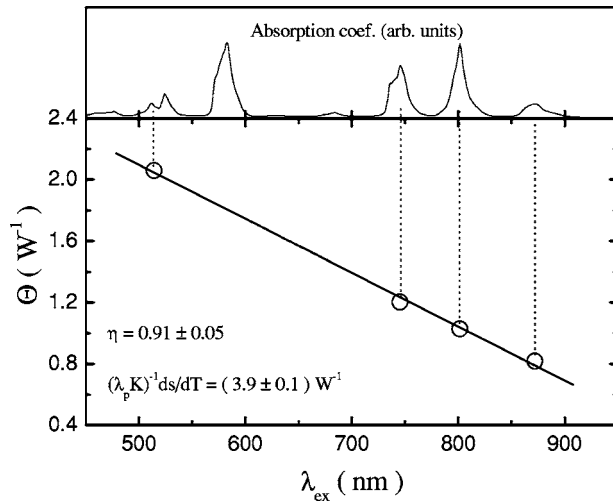


FIG. 4. Dependence of the photothermal parameter Θ with excitation beam wavelength (λ_{ex}) for Q-98 sample with $1.1 \times 10^{20} \text{ Nd}^{3+}/\text{cm}^3$. The inset shows the sample absorption spectrum with the used excitation wavelengths properly indicated.

niques such as photoacoustic^{7,8} and photocalorimetry.¹¹ Figure 4 shows the dependence of Θ versus λ_{ex} for the Q-98 glass doped with $1.1 \times 10^{20} \text{ Nd}^{3+}/\text{cm}^3$. These measurements were performed using a Ti:Sapphire laser tuned to the main Nd^{3+} near-infrared absorption lines ($\lambda_{\text{ex}}=745$, 801.5 , and 872 nm) and $\lambda_{\text{ex}}=514$ nm from an Ar^+ laser. Since the parameters η and C are obtained from the linear fit of Fig. 4 data, the MW method does not require comparison with a reference sample. Good accuracy is obtained using this approach if λ_{ex} is varied in a wide range. Therefore this method suits very well to Nd^{3+} -doped solids because all energy levels excited above the ${}^4F_{3/2}$ decay nonradiatively in cascade to this one. Consequently, λ_{ex} can be varied in a wide range without a significant change in the emission spectrum, so $\langle \lambda_{\text{em}}^{-1} \rangle$ is nearly constant (independent of λ_{ex}).^{15,24}

In the RS method it is assumed that C is the same for doped and undoped samples. Usually, a sample with negligible luminescence is used as reference so that $\eta_{\text{ref}}=0$ and $\varphi_{\text{ref}}=1$. Therefore, by measuring the TL signals of the doped (Θ_d) and undoped (Θ_{ref}) samples, φ_d is achieved through the relation $\Theta_d/\Theta_{\text{ref}}=\varphi_d=(1-\eta\langle \lambda_{\text{em}}^{-1} \rangle\lambda_{\text{ex}})$, from which η can be obtained.^{14,17} We applied the RS method in the ZBLAN and PGIZCa glasses. In this case, the reference samples (without Nd^{3+}) were doped with small amounts of CoF_2 (~ 0.1 mol %) to increase their optical absorption coefficients without presenting luminescence ($\eta_{\text{ref}}\approx 0$). The TL measurements were performed at 514 nm in resonance with the Co absorption band.¹⁶ In Tables I and II it can be seen that the η and C values obtained from the three methods (NL, MW, and RS) are in fairly good agreement.

In principle, if the $K^{-1}ds/dT$ factor is known, η can be determined from Θ without the need of a reference sample. However, generally the $K^{-1}ds/dT$ value is not available and it is difficult to have a suitable reference sample. In this perspective, the NL and MW methods are attractive because they enable the determination of η and C (and thus ds/dT) from linear fit of experimental data as in Figs. 3 and 4. In

both approaches, the accuracy is improved by increasing the number of experimental data points in the line. In the MW method, this can be achieved by covering a wide interval of excitation wavelengths. However, the use of several lasers requires new alignments of the experiment, determination of m and V parameters for each wavelength, etc. This makes the method very laborious and enhances the experimental uncertainties. Besides, the MW method fits particularly well to Nd^{3+} because this ion usually presents only one important fluorescence channel (${}^4F_{3/2}$ level). It may be unsuitable for many systems, for instance, when $\langle \lambda_{\text{em}}^{-1} \rangle$ varies much with λ_{exc} .

The main advantage of the NL method compared to the MW is its simplicity, since it requires only one λ_{ex} . So, it can be applied to several ions such as Yb, Cr, Ti, and others that must present only one emitting state and a good variation in the lifetime with concentration.³⁸ In addition, it must be noted that the η value is obtained not for one concentration only, but for a set of different concentrations, i.e., η as a function of N_i . It should be emphasized that in this approach no assumption needs to be made about the nature of the ion-ion interaction, because this information is already contained in the measured lifetime data.⁸ Also, knowledge of absolute ion concentrations is not necessary, but only of the variation of lifetime with it. Lifetimes in the order of milli or microseconds are easily measured with good accuracy, and these measurements can be performed in the same experiment setup of the TL experiment. Therefore, the NL approach does not require any kind of calibration.

The main advantage of these methods using the TL technique compared with pure optical techniques, for instance, is the ability to measure the absolute nonradiative quantum efficiency without recourse of complicated and often inaccurate absolute detector calibration procedures. Several papers have used the photoacoustic method for solids with variable degree of success. As mentioned in the introduction, Quimby and Yen⁸ first proposed the idea of comparing the photoacoustic signal with lifetime measurements. They studied Nd doped silicate glasses (ED2) obtaining, for low doping, $\eta=0.65\pm 0.05$ at $\lambda_{\text{exc}}=515$ nm and $\eta=0.75\pm 0.05$ at $\lambda_{\text{exc}}=531$ nm. These results are much lower than the value of 0.9 measured by integrating sphere and theoretically predicted. This discrepancy was attributed to excitation of different sites by the different wavelengths. However, in our view, the effect of site selection should be negligible at room temperature. Also, by using photoacoustics, Powell *et al.*³⁹ obtained $\eta=0.60$ for the Nd:YAG crystal, much lower than the expected value of 0.91.^{15,27} The problem with photoacoustic measurement for solid is the difficulty in comparing experimental data of different samples because the acoustic coupling between the sample and the sensor can vary when different samples are measured.^{1,6,8} In addition, effects of surface absorption may induce anomalous results in gas-microphone photoacoustic systems, particularly for lightly doped samples.⁷ The multiwavelength method⁶ was introduced to photoacoustic to circumvent these difficulties. With regards to calorimetric methods, their sensitivity is limited by the temperature sensors. Therefore, photothermal methods also have some drawbacks and calibration problems.

The TL technique has high sensitivity, it is accurate and simple (both theoretical and experimentally). It is also a fast

TABLE III. Spectroscopic parameters for neodymium-doped Q-98, ZBLAN, and PGIZCa laser glasses.

Parameter (units)	Materials		
	Q-98	ZBLAN	PGIZCa
A_{rad} (s^{-1})	2550	1922	2250
W_0 (s^{-1})	255 ± 188	0 ^b	107 ± 201
$\eta_0 = A_{\text{rad}} / (A_{\text{rad}} + W_0)$	0.91	1.00	0.92
C_{DD} ($10^{-39} \text{ cm}^6/\text{s}$)	4.62 ^a	3.0	2.8
C_{DA} ($10^{-41} \text{ cm}^6/\text{s}$)	0.28	1.1	1.6
C_{DA}/C_{DD} (10^{-3})	0.61	3.66	5.71
N_c (10^{20} cm^{-3})	10.6	7.3	7.3
Q (10^{20} cm^{-3})	8.8	5.3	4.7
p	2.1 ± 0.2	2.2 ± 0.2	1.9 ± 0.2

^aDatum taken from Ref. 10.

^b W_0 was fixed in zero for this sample because η is close to unit for low concentration.

response method owing to the relatively small diameter of the excitation laser. The TL response time is typically in the millisecond range (see Fig. 2), which is much faster than that with usual calorimetry (\sim minutes).¹¹ This allows the averaging of many measurements for each data point, improving the signal-to-noise ratio. Besides, the TL signal is usually not affected by surface effects. In addition, other information such as thermal diffusivity (D), the temperature coefficient of the optical path length change (ds/dT), and the TL focal distance can be determined in the same experiment.^{15,17} The main disadvantage of the NL method is the need of a set of concentrations, with significant variation of lifetimes, so that the range of the concentrations might be comparable to Q [Eq. (14)]. However, in our view, the three variations of the TL discussed in this work (NL, MW, and RS) complement each other, making TL a versatile and powerful tool for characterization of optical materials.

For laser applications, TL is an attractive technique since it also provides the thermal load parameter φ (which is related to η) and ds/dT . The TL focusing power can also be evaluated by $f^{-1} = (P_{\text{abs}} / \pi w_e^2 K) \varphi (ds/dT)$.¹⁵ According to Eq. (5), ds/dT includes the contribution of dn/dT , thermal expansion and stress. For most oxides glasses and crystals, depending on the composition/structure, the three terms in Eq. (5) are positive. On the other hand, materials with negative dn/dT , such as fluorides, are interesting to minimize ds/dT . For instance, for Q-98 $dn/dT = -4.5 \times 10^{-6} \text{ K}^{-1}$ so $|ds/dT|$ is smaller than $|dn/dT|$ due to the opposite sign of dn/dT and the other contributions to ds/dT .^{15,17,19} Similarly, fluoride glasses present negative ds/dT and also $|ds/dT| < |dn/dT|$ (for ZBLAN $dn/dT \sim -12 \times 10^{-6} \text{ K}^{-1}$). Using Q-98 data in Eq. (5) [$dn/dT = -4.5$, $\alpha(n_0 - 1)(1 + \nu) = 6.8$, and $n_0^3 Y \alpha (q_{\parallel} + q_{\perp}) / 4 = 0.1$ (all quantities in units of $\times 10^{-6} \text{ K}^{-1}$)], we calculated $ds/dT_{\text{cal}} = 2.4 \times 10^{-6} \text{ K}^{-1}$, while $ds/dT_{\text{TL}} = (1.31 \pm 0.03) \times 10^{-6} \text{ K}^{-1}$. These results are in good agreement if we suppose an uncertainty of $\sim 10\%$ in each term of Eq. (5). For laser materials it is usually desirable to have very low ds/dT . The value obtained for Q-98 is one order of magnitude lower than that of Nd:YAG ($ds/dT = 13.7$

$\times 10^{-6} \text{ K}^{-1}$).¹⁵ The main difference is that in YAG dn/dT is positive, with a magnitude about half of ds/dT .¹⁵

B. Fluorescence concentration quenching effect

In Nd-doped solids, the nonradiative decay from the $^4F_{3/2}$ level is normally attributed to the multiphonon decay, energy transfer to hydroxyl groups ($\text{Nd}^{3+} \rightarrow \text{OH}^-$) and concentration quenching (energy transfer among Nd^{3+} ions), as discussed above. Although phosphate glasses have high phonon energy ($\sim 1200 \text{ cm}^{-1}$), the multiphonon relaxation rate ($\sim 250 \text{ s}^{-1}$) is small compared to the radiative rate ($\sim 3000 \text{ s}^{-1}$).^{10,11,25} Despite the fact that these glasses are especially susceptible to contamination by water during manufacture, the η values obtained for Q-98 glasses are relatively high, in agreement

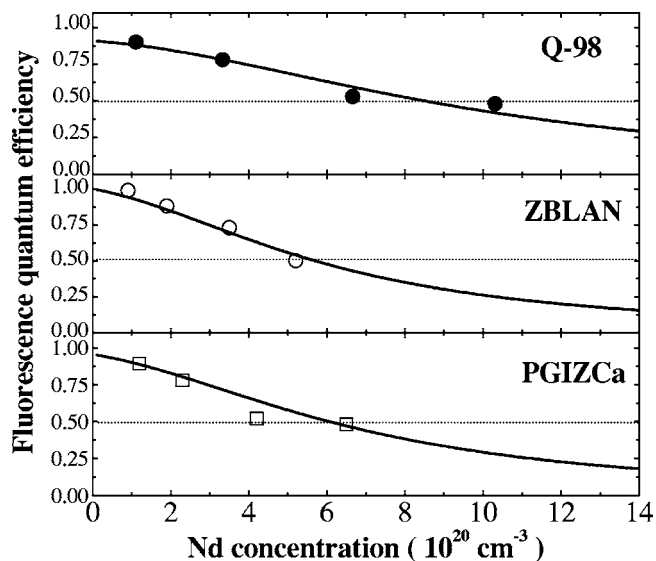


FIG. 5. Fluorescence quantum efficiency (η) obtained from the NL method, as a function of Nd concentration for Q-98, ZBLAN, and PGIZCa glasses. Solid lines are fits using Eq. (12), where the only adjustable parameters were W_0 and C_{DA} .

with previous results obtained for other phosphate glasses by photocalorimetric¹¹ and integrating-sphere¹⁰ measurements. The results achieved by TL are also in good agreement with that provided by comparison of experimental and radiative lifetimes obtained by the Judd-Ofelt analysis. The fluoride glasses (ZBLAN and PGIZCa) were prepared in dry atmosphere and no evidence of the presence of OH⁻ in the samples was detected in their infrared spectra. In addition, they present low phonon frequencies (~ 500 cm⁻¹) so $\eta \sim 1$ is expected in the low concentration regime.

Figure 5 exhibits the Nd concentration dependence of η values obtained from the NL method. The theoretical curves (solid curves) were performed using Eq. (12) with C_{DA} and W_0 as adjustable parameters. For Q-98 glass we used the $C_{DD}=4.6 \times 10^{-39}$ cm⁶/s value obtained for LG-750 phosphate glass,¹⁰ which is similar to $C_{DD}=4.7 \times 10^{-39}$ cm⁶/s for the LHG-8.³⁷ For ZBLAN and PGIZCa glasses, the C_{DD} values were achieved from the emission and absorption spectra through the Eq. (9). The lifetime data was fitted with the empirical expression given by Eq. (14) to obtain the phenomenological parameters Q and p . All glasses presented $p \sim 2$ as observed in previous works in phosphates and fluorides.^{24,25,33} All results are shown in Table III.

As expected, the behavior of both fluoride glasses (ZBLAN and PGIZCa) is similar to each other, but very different from the phosphate (Q-98). The concentration quenching found in Q-98 is much weaker than in the fluorides. Although C_{DD} is $\sim 60\%$ higher in Q-98 compared with the fluorides, the ratio C_{DA}/C_{DD} is ~ 8 times smaller. Therefore, it seems like the main difference between these two different glass families is determined by C_{DA} rather than C_{DD} . Indeed, through the theoretical analyses we noted that the quenching effect is really governed mainly by C_{DA} . In the theoretical analysis of quenching mechanisms (Sec. II C) we commented that the quantum efficient should decrease to half of its zero concentration value (η_0) for a concentration lower than N_c defined by Eq. (11). Figure 1 shows that this

concentration decreases as the ratio C_{DA}/C_{DD} increases. The Q values, obtained from the fit of fluorescence decay data by the empirical Eq. (14), are lower than the N_c calculated from C_{DA} and C_{DD} , as shown in Table III. Furthermore, a lower Q/N_c ratio is observed in fluorides compared to Q-98 due to the higher C_{DA}/C_{DD} values of the fluorides. Therefore, the experimental data corroborate the main features described in the theoretical analysis.

V. CONCLUSIONS

In conclusion, a new method for determination of η and thermo-optical coefficients of ions in solids using TL technique has been presented. A linear decrease of the normalized TL signal (Θ) with the fluorescence lifetime was observed for the three sets of samples studied (Nd-doped phosphate, fluorozirconate, and fluoroindate glasses). A very good agreement between the η and ds/dT values was obtained from the NL, MW, and RS methods. The NL methodology was not successfully implemented in photoacoustics,⁸ probably due to the difficulty of comparing data of different samples. However, this work demonstrated that NL is a simple, sensitive, and reliable method using the TL technique. The achieved results point out the TL technique as a powerful tool that can be applied for characterization of a wide class of optical materials.

The Q-98 phosphate glass has advantages over fluoride glass compositions when high Nd³⁺ concentrations are requested due to its higher $Q(N_c)$ value, which is attributed to the smaller C_{DA} and C_{DA}/C_{DD} values.

ACKNOWLEDGMENTS

The authors are thankful to CNPq and FAPESP for the financial support of this work. The authors also thank A. S. S. de Camargo for careful reading of the paper.

APPENDIX

List of variables (variable that appear only once or twice in text are not featured in this table).

D and K	thermal diffusivity and conductivity
t_c	TL characteristic response time
ds/dT	temperature coefficient of the optical path length
$I_{TL}(t)$	TL signal intensity as a function of the time
θ	probe beam phase shift induced by the thermal lens
Θ	θ normalized by the absorbed excitation power
λ_p	probe beam wavelength
φ	fraction of absorbed energy converted into heat
$\langle \nu_{em} \rangle$	average frequency of the emitted photon
ν_{ex}	frequency of the excitation photon
$N_c = [A_{rad}^2 / \pi^2 (2\pi/3)^5 C_{DD} C_{DA}]^{1/4}$	critical neodymium ion density
Q	concentration quenching factor
τ and $\tau_{rad} = 1/A_{rad}$	fluorescence and radiative lifetimes
$\eta(N) = \tau(N) / \tau_{rad}$	fluorescence quantum efficiency as a function of the ion concentration

τ^* and η^*	lifetime and fluorescence quantum efficiency of the sample taken as reference
$\Gamma = \tau / \tau^*$	parameter of lifetimes, which is concentration dependent
$I_F(t)$	fluorescence decay signal
W_0	nonradiative relaxation rate due to multiphonon emission
$\eta_0 = A_{\text{rad}} / (A_{\text{rad}} + W_0)$	fluorescence quantum efficiency in the absence of concentration quenching
dn/dT	temperature coefficient of refractive index
$C = (\lambda_p K)^{-1} ds/dT$	proportionality constant between θ and φ
N_t	total neodymium ion density
$n = N_t / N_c$	normalized concentration
C_{DD} and C_{DA}	energy transfer microparameters

*Electronic address: carlosjs@if.sc.usp.br

†Electronic address: tomaz@if.sc.usp.br

¹A. Mandelis, J. Vanniasinkam, S. Budhudu, A. Othonos, and M. Kokta, *Phys. Rev. B* **48**, 6808 (1993).

²M. Grinberg and A. Mandelis, *Phys. Rev. B* **49**, 12496 (1994).

³V. Lupei, A. Lupei, S. Georgescu, T. Taira, Y. Sato, and A. Ikesue, *Phys. Rev. B* **64**, 092102 (2001).

⁴V. Lupei and A. Lupei, *Phys. Rev. B* **61**, 8087 (2000).

⁵W. Krupke, *IEEE J. Quantum Electron.* **QE10**, 450 (1974).

⁶E. Rodríguez, J. O. Tocho, and F. Cussó, *Phys. Rev. B* **47**, 14049 (1993).

⁷A. Rosencwaig and E. A. Hildum, *Phys. Rev. B* **23**, 3301 (1981).

⁸R. S. Quimby and W. M. Yen, *Opt. Lett.* **3**, 181 (1978).

⁹L. S. Rohwer and J. E. Martin, *J. Lumin.* **115**, 77 (2005).

¹⁰J. A. Caird, A. J. Ramponi, and P. R. Staver, *J. Opt. Soc. Am. B* **8**, 1391 (1991).

¹¹A. J. Ramponi and J. A. Caird, *J. Appl. Phys.* **63**, 5476 (1988).

¹²A. Marcano O. and I. Urdaneta, *Appl. Phys. B: Lasers Opt.* **B72**, 207 (2001).

¹³A. Santhi, U. L. Kala, R. J. Nedumpara, A. Kurian, M. R. P. Kurup, P. Radhakrishnan, and V. P. N. Nampoori, *Appl. Phys. B: Lasers Opt.* **B79**, 629 (2004).

¹⁴M. L. Baesso, A. C. Bento, A. A. Andrade, J. A. Sampaio, E. Pecoraro, L. A. O. Nunes, T. Catunda, and S. Gama, *Phys. Rev. B* **57**, 10545 (1998).

¹⁵C. Jacinto, A. A. Andrade, T. Catunda, S. M. Lima, and M. L. Baesso, *Appl. Phys. Lett.* **86**, 034104 (2005).

¹⁶S. M. Lima, A. A. Andrade, R. Lebullenger, A. C. Hernandez, T. Catunda, and M. L. Baesso, *Appl. Phys. Lett.* **78**, 3220 (2001).

¹⁷S. M. Lima, J. A. Sampaio, T. Catunda, A. C. Bento, L. C. M. Miranda, and M. L. Baesso, *J. Non-Cryst. Solids* **273**, 215 (2000).

¹⁸C. Jacinto, T. Catunda, D. Jaque, and J. García-Solé, *Phys. Rev. B* **72**, 235111 (2005).

¹⁹W. Koechner, *Solid-State Laser Engineering* (Springer, New York, 1988), Vol. 1.

²⁰B. R. Judd, *Phys. Rev.* **127**, 750 (1962).

²¹G. S. Ofelt, *J. Chem. Phys.* **37**, 511 (1962).

²²J. Shen, R. D. Lowe, and R. D. Snook, *Chem. Phys.* **165**, 385

(1992).

²³M. L. Baesso, J. Shen, and R. D. Snook, *J. Appl. Phys.* **75**, 3732 (1994).

²⁴W. J. Miniscalco, in *Rare Earth Doped Fiber Lasers and Amplifiers*, edited by M. J. F. Digonnet (Stanford University Press, Stanford, 1993), pp. 19–133.

²⁵H. Ebdorff-Heidepriem, W. Seeber, and D. Ehrt, *J. Non-Cryst. Solids* **183**, 191 (1995).

²⁶Th. Förster, *Z. Naturforsch. A* **4A**, 321 (1949).

²⁷R. C. Powell, *Physics of Solid-State Laser Materials* (Springer, New York, 1998).

²⁸A. I. Burshtein, *Sov. Phys. JETP* **57**, 1165 (1983).

²⁹S. E. Stokowski, R. A. Saroyan, and M. J. Weber, Laser glass Nd-doped glass spectroscopic and physical properties, Lawrence Livermore National Laboratory Report M-095, Rev. 2, Vols. 1 and 2, 1981.

³⁰S. E. Stokowski, in *Handbook of Laser Science and Technology*, edited by M. J. Weber (CRC, Boca Raton, FL, 1982), Vol. 1, p. 1.

³¹I. M. Thomas, S. A. Payne, and G. D. Wilke, *J. Non-Cryst. Solids* **151**, 183 (1992).

³²S. A. Payne, C. D. Marshall, A. Bayramian, G. D. Wilke, and J. S. Hayden, *Appl. Phys. B: Lasers Opt.* **B61**, 257 (1995).

³³J. H. Campbell and T. I. Saratwala, *J. Non-Cryst. Solids* **263&264**, 318 (2000), and references therein.

³⁴R. Balda, J. Fernández, A. Mendioroz, J. L. Adam, and B. Boulard, *J. Phys.: Condens. Matter* **6**, 913 (1994).

³⁵S. Payne, M. L. Elder, J. H. Campbell, G. D. Wilke, and M. J. Weber, in *Solid-State Optical Materials*, edited by A. J. Bruce and B. V. Hiremath (American Ceramic Society, Westerville, OH, 1991), Vol. 28, p. 253.

³⁶C. Jacinto, S. L. Oliveira, T. Catunda, A. A. Andrade, J. D. Myers, and M. J. Myers, *Opt. Express* **13**, 2040 (2005).

³⁷J. L. Doualan, C. Maunier, D. Descamps, J. Landais, and R. Moncorgé, *Phys. Rev. B* **62**, 4459 (2000).

³⁸C. Jacinto, S. L. Oliveira, L. A. O. Nunes, T. Catunda, and M. J. V. Bell, *Appl. Phys. Lett.* **86**, 071911 (2005).

³⁹R. C. Powell, D. P. Neikirk, and D. Sardar, *J. Opt. Soc. Am.* **70**, 486 (1980).